Materials Research Bulletin 70 (2015) 106–113

Contents lists available at ScienceDirect

Materials Research Bulletin

journal homepage: www.elsevier.com/locate/matresbu

Photoredox degradation of different water pollutants (MO, RhB, MB, and Cr(VI)) using Fe–N–S-tri-doped TiO_2 nanophotocatalyst prepared by novel chemical method

Xuyao Xu, Xiaosong Zhou*, Lingling Zhang, Limei Xu, Lin Ma, Jin Luo, Mengjia Li, Lihua Zeng

School of Chemistry and Chemical Engineering, Institute of Physical Chemistry and Development Center for New Materials Engineering and Technology in Universities of Guangdong, Lingnan Normal University, Zhanjiang 524048, PR China

ARTICLE INFO

Article history:
Received 11 February 2015
Received in revised form 9 April 2015
Accepted 12 April 2015
Available online 17 April 2015

Keywords:
A. Oxides
A. Semiconductors
B. Solvothermal
D. Catalytic properties

ABSTRACT

Fe–N–S-tri-doped TiO_2 (FeNS-TiO_2) was synthesized by a simple one-step hydrothermal method. The as-synthesized samples were characterized by X-ray diffraction (XRD), transmission electron microscopy (TEM), Fourier transform infrared spectroscopy (FT-IR), and X-ray photoelectron spectroscopy (XPS). The photocatalytic activities of as-synthesized samples were tested by the oxidation of methyl orange (MO), rhodamine B (RhB), methylene blue (MB) and the reduction of aqueous Cr(VI) under visible-light ($\lambda > 420$ nm) irradiation, and compared with N-dope P25 (N-P25) and the undoped TiO_2. Besides, the effects of the coexistence of MO, RhB, and MB on FeNS-TiO_2-mediated photocatalytic reduction of aqueous Cr(VI) were also studied. The results indicated FeNS-TiO_2 displayed higher visible-light-activated photocatalytic activity than N-P25 and the undoped TiO_2. Otherwise, FeNS-TiO_2 showed the coexistence of MB enhanced the photocatalytic reduction of Cr(VI), whereas the coexistence of MO and RhB retarded the photocatalytic reduction of Cr(VI) over FeNS-TiO_2. Moreover, a possible photocatalytic mechanism is discussed.

1. Introduction

Dyes and toxic metal ions are two of the main sources of water pollutants existing in our environment. Over the decade, dyes and chromium pollution in water have become a concern due to its extensive use in chemical industries for electroplating, leather tanning, or paint processes. In general, hexavalent form of chromium is 100 times more acutely toxic than the trivalent form and thus, exposure to Cr(VI) has been demonstrated to cause cancer in the digestive tract and lungs, epigastrium pain, and nausea; whereas, Cr(III) is an essential nutrient at trace levels [1]. Hence, increasing awareness has been growing rapidly worldwide and one of the offshoots is the treatment and removal of this toxic material from such effluents to a permissible limit before discharging them into streams and rivers. For water purification treatment various technologies are in use. There are two main approaches to water pollutions removal. First approach relies on the use of cheap adsorbents [2,3] and second one employs photocatalysts like titanium dioxide.

In 2001, Asahi et al. [4] prepared nitrogen doped TiO_2 films by sputtering TiO_2 in a N_2/Ar gas mixture, and concluded that the activity for the decomposition of acetone and methylene blue improved. Since then, there are a number of publications reporting the beneficial influence of the substitution of oxygen in TiO_2 by nonmetals such as nitrogen, carbon, sulfur, and boron on bringing activity of the photocatalysts into the visible range [5–9]. However, nonmetal doping brings the serious problem of massive charge carrier recombination, which largely limits the photoactivity of doped TiO_2 under visible light [10]. The doping of various transitional metal ions into TiO_2 could shift its optical absorption edge from UV into visible light range, but a prominent change in TiO_2 band gap has not been observed [11,12]. In order to further improve the photocatalytic activity, co-doped titania with double non-metal [13–15], metal–nonmetal elements [16–18] double metal ions [19,20], and metal–semiconductor [21,22] have attracted more attention. The co-doped TiO_2 with rare-earth, transition metal, and nonmetallic elements have aroused great attention. Some studies demonstrated that the co-doping with transition metal and nonmetallic elements could effectively modify the electronic structures of TiO_2 and shift its absorption edge to a lower energy [23]. In water and wastewater treatment technologies, photocatalytic remediation was found to be suitable

---

* Corresponding author. Tel.: +86 759 3174025; fax: +86 759 3174025.
E-mail address: zxs801213@163.com (X. Zhou).

http://dx.doi.org/10.1016/j.materresbull.2015.04.020
0025-5408/© 2015 Elsevier Ltd. All rights reserved.

for aqueous solutions that contain organic compounds and reducible toxic metal ions because it was found that the photocatalytic oxidation of organics and reduction of metals are synergistic [24–26]. This observation was explained in terms of a closed redox cycle whereby the organics are destroyed by photocatalytic oxidation while the metals are removed by reduction.

In this work, visible light responsive Fe–N–S-tri-doped TiO_2 was prepared via simple one step hydrothermal process. The main advantage of the proposed route is low reaction temperature and short processing time that prevents agglomeration and grown in the formed particles, which can significantly reduce energy waste. The photocatalytic activity of the samples were evaluated by the oxidation of organic dyes (MO, RhB, and MB) and the reduction of aqueous Cr(VI) under visible irradiation. The tri-doped TiO_2 not only exhibited much higher activity than undoped TiO_2 and N-P25, but also exhibited good reusability in photocatalytic reduction of aqueous Cr(VI). The effects of the coexistence of MO, RhB, and MB on FeNS-TiO_2-mediated photocatalytic reduction of aqueous Cr (VI), and the probable reasons accounting for the photocatalytic results were also studied.

2. Experimental procedure

2.1. Preparation of catalysts

In a typical synthesis, appropriate amount of ammonium ferrous sulfate (added to ammonium ferrous sulfate: TiO_2 molar percentage of 0.2, 0.5, 1, 2, and 3 mol.%) was dissolved in 20 mL hydrochloric acid (0.1 M) to form a solution. Then 20 mL tetrabutyl titanate was added dropwise into the above solution under vigorous stirring for about 1 h to form a dispersed solution. Then, the mixture was finally transferred into a 100 mL Teflon-lined stainless steel autoclave. It was sealed tightly and maintained at 180 °C for 2 h. After that, the autoclave was allowed to cool down naturally. The products were collected, and washed with deionized water and absolute ethanol three times respectively, then dried for 12 h under vacuum at 60 °C. The resulting samples were labeled as TX (*X* denotes the molar percentage of ammonium ferrous sulfate to TiO_2, mol.%). The P25 was annealed in ammonia atmosphere at 500 °C for 4 h to obtain N-doped P25 for comparison, and were denoted as N-P25.

2.2. Characterization

XRD analysis was performed on a D/Max-2550 X-ray diffractometer with monochromatized CuKα radiation ($\lambda = 0.1540562$ nm). TEM was recorded on a transmission electron microscopy (TEM, JEOL JEM-200CX). The UV–vis light absorption spectra of as-synthesized samples were obtained from a Hitachi UV-3010 spectrophotometer, equipped with an integrating sphere assembly and using the diffuse reflection method and $BaSO_4$ as a reference to measure all the samples. FT-IR spectra of the samples were recorded on a Nicolet Impact 360 spectrometer. The chemical nature of N, S, and Fe in TiO_2 was studied using X-ray photoelectron spectroscopy (XPS) in Krato Axis Ultra DLD spectrometer with Al Ka X-ray ($h\nu = 1486.6$ eV) at 15 kV and 150 W. The binding energy was referenced to C 1s line at 284.6 eV for calibration.

2.3. Photocatalytic tests

Photocatalytic properties of the obtained products were tested by the oxidation of organic dyes (MO, RhB, and MB) and the reduction of aqueous Cr(VI) under visible irradiation in a 250 mL cylindrical quartz reactor equipped with a water circulation facility. A 500 W Xe lamp with a light filter cutting off the short wavelength below 420 nm was used as light source. The distance between the light source and the reactor was 20 cm. All the photocatalytic experiments were performed at ambient temperature. In a typical experiment, 0.2 g catalyst was merged into 200 mL dyes solution and $K_2Cr_2O_7$ aqueous solution, and the initial concentration was 20 mg/L and 5 mg/L, respectively. Prior to photoreaction, the solution was stirred in the dark for 1 h to reach adsorption–desorption equilibrium. During illumination, about 3 mL of suspension was taken from the reactor at a scheduled interval and centrifuged at 12,000 rpm for 15 min. The concentration of solution in the supernatant was analyzed by measuring the absorbance with a UV–vis spectrophotometer. The Cr(VI) contents were determined colorimetrically using the standard diphenylcarbazide method with a detection limit of 0.005 mg/L [24,27].

3. Results and discussion

3.1. XRD and TEM analysis

XRD patterns of the samples are shown in Fig. 1. The major crystalline phase detected in all samples is anatase. As shown in Fig. 1, the samples show trace amount of brookite phase. This response probably because the chloride ion promotes the crystallization of brookite [28]. It should be noteworthy that no peaks related to the doping species could be observed in the XRD spectra. One of the reason might be that the concentration of dopants was so low and could not be detected by XRD. The other was that the dopants were incorporated into the structures of TiO_2 and substituted the lattice titanium and oxygen atoms or located at the interstitial site. Further, by using the Debye–Scherrer equation, the average crystallite sizes of pure TiO_2 and T3 sample were found to be 19 and 8 nm, respectively.

The crystallite sizes of the as-synthesized TiO_2 samples were also evaluated by TEM. As shown in Fig. 2(A), the average diameter of pure TiO_2 nanoparticles was about 20 nm, while the T3 sample was about 9.0 nm (see Fig. 2(B)), which was consistent well with the calculated from the XRD characterization.

3.2. UV–vis diffuse reflectance spectra

The optical properties of as-synthesized TiO_2 samples were investigated by UV–vis diffuse reflectance spectra and are shown in Fig. 3(A). It is apparent that the diffuse reflectance spectra of all the doped samples have extended a red shift and increased absorbance in the visible range. It is expected that nitrogen and sulfur doping contributed to the red shift because of the narrowing

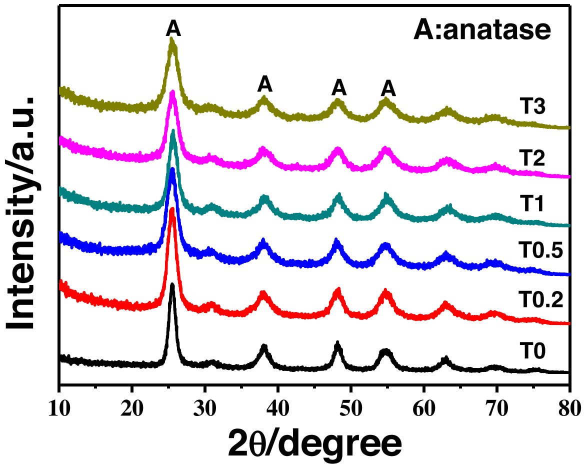

Fig. 1. XRD patterns of the as-prepared samples.